Scalable Solvers for Cardiac Electromechanical Models

Luca F. Pavarino
Università di Milano, Italy

P. Colli Franzone, Università di Pavia, Italy
S. Scacchi, Università di Milano, Italy
S. Zampini, KAUST, Saudi Arabia

Workshop on PDE's and Biomedical Applications
Lisbon, 4 - 6 December 2014

Coupled multiphysics in cardiac modeling

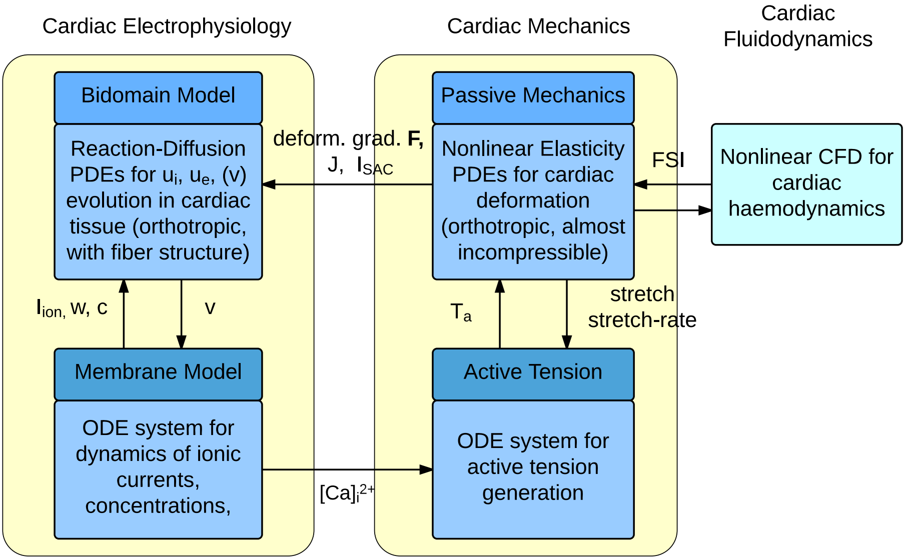

1. Cardiac bioelectrical model: the Bidomain system

Reaction-Diffusion system of degenerate parabolic PDEs:

- Given $I_{app}^{i,e}$ (applied current), v_0, w_0 (initial conditions)
- find u_i, u_e =intra and extracellular potentials,
  (and $v = u_i - u_e$ = transmembrane potential),
  w =gating variables and c =ion concentrations such that:

Reaction-Diffusion system of degenerate parabolic PDEs:

- Given $I_{app}^{i,e}$ (applied current), v_0, w_0 (initial conditions)
- find u_i, u_e =intra and extracellular potentials,
  (and $v = u_i - u_e$ = transmembrane potential),
  w =gating variables and c =ion concentrations such that:

Bidomain system (P-P formulation):

$$\rho C_m \frac{\partial v}{\partial t} - \mathrm{div}(D_i \nabla u_i) + \rho I_{ion}(v, w, c) = -I_{app}^i \qquad \text{in } \Omega \times (0, T)$$

$$-\rho C_m \frac{\partial v}{\partial t} - \mathrm{div}(D_e \nabla u_e) - \rho I_{ion}(v, w, c) = I_{app}^e \qquad \text{in } \Omega \times (0, T)$$

$$\frac{\partial w}{\partial t} = R(v, w), \qquad \frac{\partial c}{\partial t} = S(v, w, c) \qquad \text{in } \Omega \times (0, T)$$

with 0 Neumann b.c. for u_i, u_e, initial conditions for v, w, c

ρ = ratio membrane area/tissue volume, C_m = surface capacitance

Colli Franzone, LFP, Scacchi, Mathematical Cardiac Electrophysiology, Springer, 2014

Conductivity tensors:

$$D_{i,e}(\mathbf{x}) = \sigma_l^{i,e}\ \mathbf{a}_l\mathbf{a}_l^T + \sigma_n^{i,e}\ \mathbf{a}_n\mathbf{a}_n^T + \sigma_t^{i,e}\ \mathbf{a}_t\mathbf{a}_t^T$$

$\sigma_l^{i,e}, \quad \sigma_n^{i,e}, \quad \sigma_t^{i,e} \quad =$ conductivity coefficients along directions
$\mathbf{a}_l$: along fiber, $\mathbf{a}_n$: normal to lamina, $\mathbf{a}_t$ = tangent to lamina
$\Rightarrow$ electrical conductivity depends on fiber and laminar structure

Conductivity tensors:

$$D_{i,e}(\mathbf{x}) = \sigma_l^{i,e}\ \mathbf{a}_l \mathbf{a}_l^T + \sigma_n^{i,e}\ \mathbf{a}_n \mathbf{a}_n^T + \sigma_t^{i,e}\ \mathbf{a}_t \mathbf{a}_t^T$$

$\sigma_l^{i,e}, \quad \sigma_n^{i,e}, \quad \sigma_t^{i,e} \quad$ = conductivity coefficients along directions
$\mathbf{a}_l$: along fiber, $\mathbf{a}_n$: normal to lamina, $\mathbf{a}_t$ = tangent to lamina
$\Rightarrow$ electrical conductivity depends on fiber and laminar structure

Ionic membrane model:

Ionic current I_{ion} and functions R, S in ODE systems are given by the chosen ionic membrane model:

- LR1, LRd00, LRd07, ... (ventricular, guinea pig)
- Shannon04, Mahajan07, ... (ventricular, rabbit)
- Ten Tusscher04, O'Hara-Rudy11, ... (ventricular, human)

2. Mechanical models of the cardiac tissue

Cardiac tissue modeled as a nonlinear elastic material. Notations:

- $\mathbf{X} = (X_1, X_2, X_3)^T \in \widehat{\Omega}$ undeformed cardiac domain
- $\mathbf{x} = (x_1, x_2, x_3)^T \in \Omega$ deformed cardiac domain
- $\mathbf{F}(\mathbf{X}, t) = \{F_{ij} = \frac{\partial x_i}{\partial X_j} \quad i, j = 1, 2, 3\}$ deformation gradient tensor and $J(\mathbf{X}, t) = det(\mathbf{F}(\mathbf{X}, t))$
- $\mathbf{C} = \mathbf{F}^T\mathbf{F}$ Cauchy-Green deformation tensor
- $\mathbf{E} = \frac{1}{2}(\mathbf{C} - \mathbf{I})$ Lagrange-Green strain tensor ($\mathbf{I}$ identity)
- $\mathrm{Div}, \mathrm{div}$ (Grad, ∇) the material, spatial divergence (gradient)

2. Mechanical models of the cardiac tissue

Cardiac tissue modeled as a nonlinear elastic material. Notations:

- $\mathbf{X} = (X_1, X_2, X_3)^T \in \widehat{\Omega}$ undeformed cardiac domain
- $\mathbf{x} = (x_1, x_2, x_3)^T \in \Omega$ deformed cardiac domain
- $\mathbf{F}(\mathbf{X}, t) = \{F_{ij} = \frac{\partial x_i}{\partial X_j} \quad i, j = 1, 2, 3\}$ deformation gradient tensor and $J(\mathbf{X}, t) = det(\mathbf{F}(\mathbf{X}, t))$
- $\mathbf{C} = \mathbf{F}^T\mathbf{F}$ Cauchy-Green deformation tensor
- $\mathbf{E} = \frac{1}{2}(\mathbf{C} - \mathbf{I})$ Lagrange-Green strain tensor ($\mathbf{I}$ identity)
- $\mathrm{Div}, \mathrm{div}\ (\mathrm{Grad}, \nabla)$ the material, spatial divergence (gradient)

Equilibrium equations

deformed body	undeformed body
$\mathrm{div}\ \boldsymbol{\sigma} = 0, \qquad \mathbf{x} \in \Omega,$	$\mathrm{Div}(\mathbf{SF}) = 0 \qquad \mathbf{X} \in \widehat{\Omega},$

with $\mathbf{S} = \{S_{ij}\} = J\mathbf{F}^{-1}\boldsymbol{\sigma}\mathbf{F}^{-T}$ = 2nd Piola-Kirchhoff stress tensor

The stress tensor: passive and active components

a) Active stress assumption: $\mathbf{S}$ is the sum of

- an active biochemically generated component $\mathbf{S}^{act}$,
- a passive elastic component $\mathbf{S}^{pas}$,
- a volume component $\mathbf{S}^{vol}$,

$$\mathbf{S} = \mathbf{S}^{act} + \mathbf{S}^{pas} + \mathbf{S}^{vol}$$

Most used in the literature: Nash and Hunter 2000, Vetter and McCulloch 2000; Kerckhoffs et al. 2003; Nash and Panfilov 2004; Sainte-Marie 2006; Pathmanathan and Whiteley 2009; Gotkepe and Kuhl 2010; Jie, Gurev and Trayanova 2010; Niederer, Nash, Hunter, Smith 2011; ...

The stress tensor: passive and active components

a) Active stress assumption: $\mathbf{S}$ is the sum of

- an active biochemically generated component $\mathbf{S}^{act}$,
- a passive elastic component $\mathbf{S}^{pas}$,
- a volume component $\mathbf{S}^{vol}$,

$$\mathbf{S} = \mathbf{S}^{act} + \mathbf{S}^{pas} + \mathbf{S}^{vol}$$

Most used in the literature: Nash and Hunter 2000, Vetter and McCulloch 2000; Kerckhoffs et al. 2003; Nash and Panfilov 2004; Sainte-Marie 2006; Pathmanathan and Whiteley 2009; Gotkepe and Kuhl 2010; Jie, Gurev and Trayanova 2010; Niederer, Nash, Hunter, Smith 2011; ...

b) Active strain alternative assumption: multiplicative strategy for combining the passive $\mathbf{S}^{pas}$ and active $\mathbf{S}^{act}$ components,

Cherubini et al 2008, then used by Ambrosi et al. 2011, Nobile, Quarteroni and Ruiz-Baier 2012, Rossi et al. 2012...

active stress vs. active strain

canine biventricular geometry from Ayache et al. 2007,
orthotropic constitutive law from Holzapfel & Ogden 2009

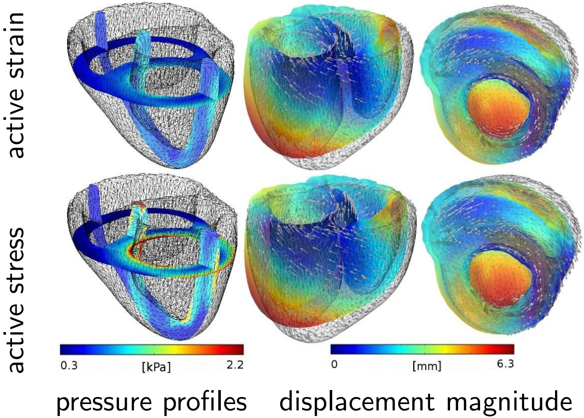

Rossi, Ruiz-Baier, LFP, Quarteroni, *IJNMBE* 28, 2012

2.1 Models of active tension

a) $T_a = T_a(t, Ca_i)$ depends only on Ca_i

$$\frac{dT_a}{dt} = \epsilon(Ca_i)\ [\eta([Ca_i - Ca_i^{rest}) - T_a]$$

where $\epsilon(Ca_i) = \epsilon_0 + (\epsilon_\infty - \epsilon_0)\exp(-\exp(-\xi(Ca_i - Ca_i^{rest})))$

(Kuhl et al., PBMB 2012, smooth variant of Nash, Panfilov, IJNMBE 2004)

2.1 Models of active tension

a) $T_a = T_a(t, Ca_i)$ depends only on Ca_i

$$\frac{dT_a}{dt} = \epsilon(Ca_i)\ [\eta([Ca_i - Ca_i^{rest}) - T_a]$$

where $\epsilon(Ca_i) = \epsilon_0 + (\epsilon_\infty - \epsilon_0)\exp(-\exp(-\xi(Ca_i - Ca_i^{rest})))$

(Kuhl et al., PBMB 2012, smooth variant of Nash, Panfilov, IJNMBE 2004)

b) $T_a = T_a(Ca_i, \lambda)$ depends on Ca_i and fiber stretch $\lambda = \sqrt{\hat{\mathbf{a}}_l^T \mathbf{C} \hat{\mathbf{a}}_l}$

$$T_a = \frac{Ca_i^n}{Ca_i^n + C_{50}^n}\ T_a^{max}(1 + \eta(\lambda - 1))$$

(Hunter et al. 1997)

2.1 Models of active tension

a) $T_a = T_a(t, Ca_i)$ depends only on Ca_i

$$\frac{dT_a}{dt} = \epsilon(Ca_i)\,[\eta([Ca_i - Ca_i^{rest}) - T_a]$$

where $\epsilon(Ca_i) = \epsilon_0 + (\epsilon_\infty - \epsilon_0)\exp(-\exp(-\xi(Ca_i - Ca_i^{rest})))$

(Kuhl et al., PBMB 2012, smooth variant of Nash, Panfilov, IJNMBE 2004)

b) $T_a = T_a(Ca_i, \lambda)$ depends on Ca_i and fiber stretch $\lambda = \sqrt{\hat{\mathbf{a}}_l^T \mathbf{C} \hat{\mathbf{a}}_l}$

$$T_a = \frac{Ca_i^n}{Ca_i^n + C_{50}^n}\; T_a^{max}(1 + \eta(\lambda - 1))$$

(Hunter et al. 1997)

c) $T_a = T_a\left(Ca_i, \lambda, \frac{d\lambda}{dt}\right)$ depends on Ca_i, stretch and stretch-rate

system of 4 ODEs (Land et al. J. Physiol, 2012)

Active stress tensor

We assume that the generated active force acts only in the direction of the fiber (Pathmanathan et al. 2009, Whiteley 2007, Goktepek et al. 2010) hence the active Cauchy stress is expressed as

$$\boldsymbol{\sigma}^{act}(\mathbf{x}, t) = J^{-1} \; T_a \; \mathbf{a}_l(\mathbf{x}) \otimes \mathbf{a}_l(\mathbf{x}),$$

with $\mathbf{a}_l(\mathbf{x})$ = unit vector parallel to the local fiber direction l and T_a = the active fiber stress related to the deformed domain.

Active stress tensor

We assume that the generated active force acts only in the direction of the fiber (Pathmanathan et al. 2009, Whiteley 2007, Goktepek et al. 2010) hence the active Cauchy stress is expressed as

$$\boldsymbol{\sigma}^{act}(\mathbf{x},t) = J^{-1}\ T_a\ \mathbf{a}_l(\mathbf{x}) \otimes \mathbf{a}_l(\mathbf{x}),$$

with $\mathbf{a}_l(\mathbf{x})$ = unit vector parallel to the local fiber direction l and T_a = the active fiber stress related to the deformed domain.

Then, the second Piola-Kirchhoff active stress component is:

$$\mathbf{S}^{act}(\mathbf{X},t) = J\ \mathbf{F}^{-1}\boldsymbol{\sigma}^{act}\mathbf{F}^{-T} = \ \hat{T}_a\ \frac{\hat{\mathbf{a}}_l \otimes \hat{\mathbf{a}}_l}{\hat{\mathbf{a}}_l^T\,\mathbf{C}\,\hat{\mathbf{a}}_l}, \qquad (\mathbf{a}_l = \frac{\mathbf{F}\hat{\mathbf{a}}_l}{|\mathbf{F}\hat{\mathbf{a}}_l|})$$

Active components in the directions $\mathbf{a}_t, \mathbf{a}_n$ can be also considered.

2.2 Passive component

The passive myocardium is modeled as an almost-incompressible transversely isotropic hyperelastic material with the exponential strain-energy function (Vetter and McCulloch 2000):

$$W^{pas} = \frac{1}{2} c \left(e^{Q} - 1 \right),$$

$$Q = b_1 E_{ll}^2 + b_2 (E_{tt}^2 + E_{nn}^2 + 2E_{tn}^2) + 2b_3 (E_{lt}^2 + E_{ln}^2),$$

where $E_{rs} = \hat{\mathbf{a}}_r^T \mathbf{E} \, \hat{\mathbf{a}}_s, \quad r, s \in \{l, t, n\}$ with local fiber coordinate system with directions l (along fiber), n (across fiber), t (radial transmural)

2.2 Passive component

The passive myocardium is modeled as an almost-incompressible transversely isotropic hyperelastic material with the exponential strain-energy function (Vetter and McCulloch 2000):

$$W^{pas} = \frac{1}{2} c \left(e^{Q} - 1 \right),$$

$$Q = b_1 E_{ll}^2 + b_2 (E_{tt}^2 + E_{nn}^2 + 2E_{tn}^2) + 2b_3 (E_{lt}^2 + E_{ln}^2),$$

where $E_{rs} = \hat{\mathbf{a}}_r^T \mathbf{E} \, \hat{\mathbf{a}}_s, \quad r, s \in \{l, t, n\}$ with local fiber coordinate system with directions l (along fiber), n (across fiber), t (radial transmural)

Almost-incompressibility enforced by adding to the strain energy a volumetric term depending on a bulk modulus K :

$$W^{vol} = K \left(\sqrt{J} - 1 \right)^2 \text{ or } W^{vol} = K \frac{J^2 - 1 - 2 lnJ}{4}$$

Passive and volumetric stress tensors

In the local fiber coordinate system of the reference configuration, the passive and volumetric components of the 2nd Piola - Kirchhoff stress tensor are

$$S_{rs}^{pas} = \frac{1}{2}\left(\frac{\partial W^{pas}}{\partial E_{rs}} + \frac{\partial W^{pas}}{\partial E_{sr}}\right), \quad r, s \in \{l, t, n\},$$

$$S_{rs}^{vol} = \frac{1}{2}\left(\frac{\partial W^{vol}}{\partial E_{rs}} + \frac{\partial W^{vol}}{\partial E_{sr}}\right), \quad r, s \in \{l, t, n\}.$$

2.3 The Bidomain model on the undeformed domain $\hat{\Omega}$

P-P formulation

$$\begin{cases} \chi\left(C_m \frac{\partial v}{\partial t} + I_{ion}^{me}\right) - \frac{1}{J}\mathrm{Div}\left(J\,\mathbf{F}^{-1} D_i \mathbf{F}^{-T}\mathrm{Grad}\, u_i\right) = 0 \\ -\chi\left(C_m \frac{\partial v}{\partial t} + I_{ion}^{me}\right) - \frac{1}{J}\mathrm{Div}\left(J\,\mathbf{F}^{-1} D_e \mathbf{F}^{-T}\mathrm{Grad}\, u_e\right) = I_{app}^{e} \\ \frac{\partial w}{\partial t} = R(v,w), \;\; \frac{\partial c}{\partial t} = S(v,w,c), \end{cases}$$

Mechano-electric feedback: deformation affects bioelectric phenomena, mostly during the repolarization phase.

- Conductivity coefficients modified with deformation gradient tensor $\mathbf{F}(\mathbf{X},t)$ and $J(\mathbf{X},t)$
- ionic term $I_{ion}^{me}(v,w,c,\lambda) = I_{ion} + I_{SAC}$ augmented with the stretch-activated current $I_{SAC}(v,\lambda)$
- possible presence of a convective term dependent on the velocity field $\mathbf{V} = \frac{\partial \mathbf{x}(\mathbf{X},\mathbf{t})}{\partial \mathbf{t}}$ of the deformation field.

3. Discrete problem

3.1 Splitting and IMEX method in time: given v^n, w^n, c^n, $\mathbf{x}^n$, $\mathbf{F}^n$,

a. Solve the membrane model with a first order IMEX method

to compute the new w^{n+1}, c^{n+1}, in particular Ca_i^{n+1}

3. Discrete problem

3.1 Splitting and IMEX method in time: given v^n, w^n, c^n, $\mathbf{x}^n$, $\mathbf{F}^n$,

a. Solve the membrane model with a first order IMEX method

to compute the new w^{n+1}, c^{n+1}, in particular Ca_i^{n+1}

b. Solve the coupled active tension and mechanical models

to compute new deformed coordinates $\mathbf{x}^{n+1}$, providing the new deformation gradient tensor $\mathbf{F}^{n+1}$ and active tension T_a^{n+1},

3. Discrete problem

3.1 Splitting and IMEX method in time: given v^n, w^n, c^n, $\mathbf{x}^n$, $\mathbf{F}^n$,

a. Solve the membrane model with a first order IMEX method

to compute the new w^{n+1}, c^{n+1}, in particular Ca_i^{n+1}

b. Solve the coupled active tension and mechanical models

to compute new deformed coordinates $\mathbf{x}^{n+1}$, providing the new deformation gradient tensor $\mathbf{F}^{n+1}$ and active tension T_a^{n+1},

c. Solve the Bidomain system. Given w^{n+1}, c^{n+1}, $\mathbf{x}^{n+1}$, $\mathbf{F}^{n+1}$,

compute the new electric potentials u_i^{n+1}, u_e^{n+1},
$v^{n+1} = u_i^{n+1} - u_e^{n+1}$

3. Discrete problem

3.1 Splitting and IMEX method in time: given v^n, w^n, c^n, $\mathbf{x}^n$, $\mathbf{F}^n$,

a. Solve the membrane model with a first order IMEX method

to compute the new w^{n+1}, c^{n+1}, in particular Ca_i^{n+1}

b. Solve the coupled active tension and mechanical models

to compute new deformed coordinates $\mathbf{x}^{n+1}$, providing the new deformation gradient tensor $\mathbf{F}^{n+1}$ and active tension T_a^{n+1},

c. Solve the Bidomain system. Given w^{n+1}, c^{n+1}, $\mathbf{x}^{n+1}$, $\mathbf{F}^{n+1}$,

compute the new electric potentials u_i^{n+1}, u_e^{n+1},
$v^{n+1} = u_i^{n+1} - u_e^{n+1}$

3.2 $\mathbf{Q}^1$ isoparametric FEM in space, structured meshes

3.3 Parallel Mechanical/Bidomain solvers at each time step

- mechanical problem (nonlinear system):
  - outer iteration: Newton method
  - inner iteration (Jacobian system): GMRES, preconditioned by
  - preconditioner: Algebraic Multigrid (BoomerAMG, Henson and Yang, 2002) or BDDC

3.3 Parallel Mechanical/Bidomain solvers at each time step

- mechanical problem (nonlinear system):
  - outer iteration: Newton method
  - inner iteration (Jacobian system): GMRES, preconditioned by
  - preconditioner: Algebraic Multigrid (BoomerAMG, Henson and Yang, 2002) or BDDC
- Bidomain model (linear system):
  - Preconditioned Conjugate Gradient (PCG) method
  - preconditioner: Multilevel Hybrid Schwarz or BDDC

3.3 Parallel Mechanical/Bidomain solvers at each time step

- mechanical problem (nonlinear system):
  - outer iteration: Newton method
  - inner iteration (Jacobian system): GMRES, preconditioned by
  - preconditioner: Algebraic Multigrid (BoomerAMG, Henson and Yang, 2002) or BDDC
- Bidomain model (linear system):
  - Preconditioned Conjugate Gradient (PCG) method
  - preconditioner: Multilevel Hybrid Schwarz or BDDC
- Parallel libraries: MPI, PETSc (Argonne NL), BoomerAMG (within HYPRE library, Lawrence Livermore NL)

3.3 Parallel Mechanical/Bidomain solvers at each time step

- mechanical problem (nonlinear system):
  - outer iteration: Newton method
  - inner iteration (Jacobian system): GMRES, preconditioned by
  - preconditioner: Algebraic Multigrid (BoomerAMG, Henson and Yang, 2002) or BDDC
- Bidomain model (linear system):
  - Preconditioned Conjugate Gradient (PCG) method
  - preconditioner: Multilevel Hybrid Schwarz or BDDC
- Parallel libraries: MPI, PETSc (Argonne NL), BoomerAMG (within HYPRE library, Lawrence Livermore NL)
- Computational platforms:
  - local clusters at Univ. of Milan/Pavia ($O(10^2)$ cores)
  - SP6 and Fermi BG\Q of CINECA ($O(10^3 - 10^5)$ cores)

3.4 Multilevel Additive Schwarz (MAS) preconditioners

- $\mathcal{T}_k$, $k = 0, ..., L-1$: nested triangulations of Ω, $\mathcal{T}_{L-1} = \mathcal{T}_h$

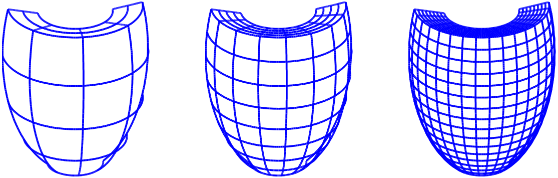

$\mathcal{T}_0 = 4 \cdot 4 \cdot 2$ $\qquad$ $\mathcal{T}_1 = 2\mathcal{T}_0$ $\qquad$ $\mathcal{T}_2 = 2\mathcal{T}_1 \cdots$

- $\mathcal{T}_k = \{\Omega_{km}\}_{m=1}^{N_k}$, subdomains with overlap δ_k and diameter H_k

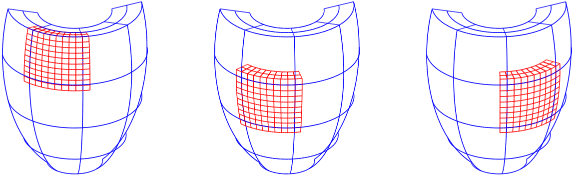

Ω_{k2} $\qquad$ Ω_{k6} $\qquad$ Ω_{k7} $\qquad \dots$

Matrix form of MAS(L) preconditioner $\mathcal{P}_{MAS}^{-1}$:

$$\mathcal{P}_{MAS}^{-1} = R_0^T B_0^{-1} R_0 + \sum_{k=1}^{L-1} \sum_{m=1}^{N_k} R_{km}^T B_{km}^{-1} R_{km}$$

where

- B_{km} = local bidomain matrix on Ω_{km} (level k, subdomain m)
- R_{km} = restriction matrix to nodes in Ω_{km}

- B_0 = coarse bidomain matrix on $\mathcal{T}_0$
- R_0 = restriction matrix to nodes in coarse mesh $\mathcal{T}_0$

Bidomain MAS preconditioners

Theorem: MAS(L) convergence rate bounds

The condition number of the Multilevel Additive Schwarz operator $\mathcal{P}_{MAS}^{-1}\mathcal{B}$ for the Bidomain system is bounded by

$$\boxed{\kappa_2(\mathcal{P}_{MAS}^{-1}\mathcal{B}) \leq C \max_{k=1,\ldots,L-1} \left(1 + \frac{H_k}{\delta_k}\right)}$$

with C constant independent of:
L = number of levels, δ_k = overlap at level k,
h_k = mesh size on level k, $H_k (= h_{k-1})$ subdomain diam. at level k.

Bidomain MAS preconditioners

Theorem: MAS(L) convergence rate bounds

The condition number of the Multilevel Additive Schwarz operator $\mathcal{P}_{MAS}^{-1}\mathcal{B}$ for the Bidomain system is bounded by

$$\boxed{\kappa_2(\mathcal{P}_{MAS}^{-1}\mathcal{B}) \leq C \max_{k=1,\dots,L-1} \left(1 + \frac{H_k}{\delta_k}\right)}$$

with C constant independent of:

L = number of levels, δ_k = overlap at level k,

h_k = mesh size on level k, $H_k (= h_{k-1})$ subdomain diam. at level k.

Proof + numerical results in

LFP, S. Scacchi, SIAM J. Sci. Comp., 31 (1), 2008

Analogous scalability bound holds for decoupled NKS MAS(2)

M. Munteanu, LFP, S. Scacchi, SIAM J. Sci. Comp., 31 (5), 2009

and for PE formulation with/without block-preconditioners

LFP, S. Scacchi, SIAM J. Sci. Comp., 33 (4), 2011

A) MAS(4) scalability on BlueGene/Q (Cineca),
overlap $\delta = 1$, ILU(0) local solvers
local mesh size 32^3 (+ overlap), 10 time steps, $\Delta t = 0.05$ ms.

procs	*dof*	coupled			decoupled		
		$\kappa_2 = \lambda_M/\lambda_m$	*it*	*time*	$\kappa_2 = \lambda_M/\lambda_m$	*it*	*time*
64	4.3e+6	41.8=8.7/2.1e-1	43	5.6	15.5=4.5/2.9e-1	29	1.8+1.1=2.9
128	8.5e+6	33.4=6.8/2.0e-1	39	5.6	14.9=4.5/3.0e-1	28	2.0+1.0=2.9
256	1.7e+7	36.4=6.8/1.9e-1	40	5.7	15.4=4.5/2.9e-1	28	1.9+1.0=3.0
512	3.3e+7	27.4=5.2/1.9e-1	36	5.5	14.3=4.4/3.0e-1	28	2.0+1.0=3.0
1K	6.7e+7	29.5=5.2/1.7e-1	36	5.7	14.4=4.4/3.1e-1	28	2.2+1.0=3.2
2K	1.3e+8	27.6=5.1/1.8e-1	34	8.5	13.2=4.3/3.3e-1	27	2.9+1.7=4.6
4K	2.7e+8	28.9=5.1/1.8e-1	34	16.3	13.2=4.3/3.3e-1	27	5.6+3.6=9.2
8K	5.4e+8	25.0=5.1/2.0e-1	32	16.5	12.4=4.3/3.5e-1	26	5.9+3.7=9.7
16K	1.1e+9	26.5=5.1/1.9e-1	32	17.4	12.4=4.3/3.5e-1	26	6.2+3.8=10.1
32K	2.1e+9	out of memory			12.0=4.3/3.6e-1	26	6.9+3.9=10.8

plots from previous table:

condition number

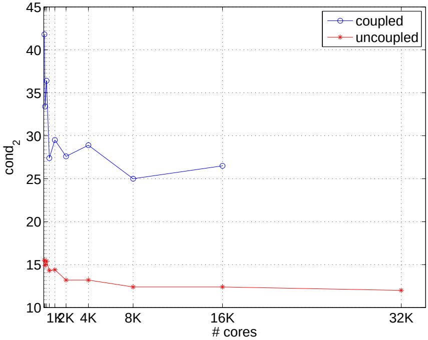

cpu time

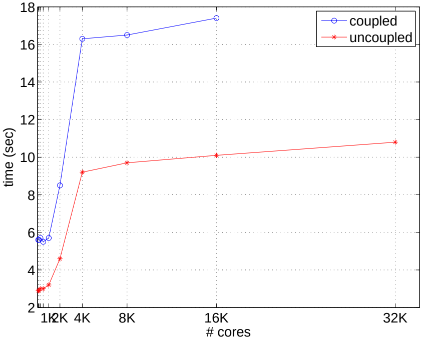

4.2 Mechanical solver: AMG weak scalability

- Simulation of 1.5 *ms* (30 time steps of $\tau = 0.05$ *ms*) during the plateau phase on truncated ellipsoidal domains.
- Fixed local mechanical dof per subdomain: 13 476

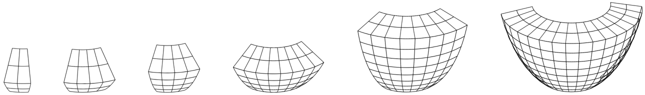

4.2 Mechanical solver: AMG weak scalability

- Simulation of 1.5 *ms* (30 time steps of $\tau = 0.05$ *ms*) during the plateau phase on truncated ellipsoidal domains.
- Fixed local mechanical dof per subdomain: 13 476

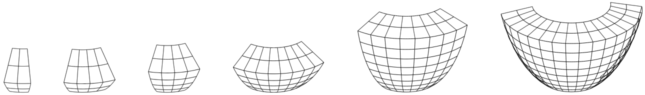

Mechanical solver - AMG preconditioner				
procs	dof	outer iter. Newton	inner iter. GMRES	CPU time
8	107 811	2	42	12.06
27	352 947	2	42	16.70
64	823 875	2	39	23.45
125	1 594 323	2	39	30.66
216	2 738 019	2	40	49.12
512	6 440 067	2	40	75.09

Mechanical solver: AMG strong scalability

Fixed global mechanical dof: 823 872

Mechanical solver - AMG preconditioner					
procs	local dof	nit	lit	time	speedup
8	102 984	2	41	110.84	-
16	51 492	2	40	63.61	1.74 (2)
32	25 746	2	41	34.64	3.20 (4)
64	12 873	2	39	23.26	4.76 (8)
128	6 436	2	40	16.08	6.89 (16)
256	3 218	2	40	15.50	7.15 (32)
512	1 609	2	41	16.97	6.53 (64)

nit = Newton iterations

it = CG iteration counts

time = CPU time in sec. to solve mechanical pb.

Fixed local Bidomain dof per subdomain: 68 656

Bidomain solver - MHS(4) preconditioner							
		non-deforming ($\mathbf{C} = \mathbf{I}$)			deforming		
procs	dof	κ_2	it	time	κ_2	it	time
8	549 250	1.11	3	1.05	1.11	3	1.31
27	1 825 346	1.11	3	1.19	1.12	3	1.17
64	4 293 378	1.12	3	1.23	1.13	3	1.21
125	8 346 562	1.13	3	1.31	1.18	4	1.49
216	14 378 114	1.18	4	1.55	1.20	4	1.55
343	22 781 250	1.15	4	1.62	1.17	4	1.66
512	33 949 186	1.14	4	1.96	1.17	4	1.67

κ_2 = average condition number per time step
it = average CG iteration counts per time step
time = average CPU time in seconds to solve one Bidomain linear system

Bidomain - Multilevel Hybrid Schwarz strong scalability

Fixed global Bidomain dof: 4 293 376

Bidomain solver - MHS(4) preconditioner					
procs	local dof	κ_2	it	time	speedup
8	536 672	1.13	3	9.18	-
16	268 336	1.13	3	5.16	1.78 (2)
32	134 168	1.14	3	2.62	3.50 (4)
64	67 084	1.15	3	1.30	7.06 (8)
128	33 542	1.16	4	0.72	12.75 (16)
256	16 771	1.19	4	0.48	19.12 (32)
512	8 385	1.20	4	0.26	35.31 (64)

4.4 Whole heartbeat: ventricular wedge deformation + v

4.4 Whole heartbeat: ventricular wedge deformation + v

endo

4.4 Whole heartbeat: ventricular wedge deformation + v

endo

transmural

Whole heartbeat

Simulation of 500 ms on a truncated half ellipsoidal domain modeling half left ventricle. Number of processors = 24

Mechanical Solver: dof = 32967, time step = 0.25 ms

Prec.	*Newton nit*	*Total nit*	*GMRES it*	*Total it*	*time cpu*	*Tot cpu*
AMG	3	7031	796	6.5 ML	28.42s	15h 47m

Whole heartbeat

Simulation of 500 ms on a truncated half ellipsoidal domain modeling half left ventricle. Number of processors = 24

Mechanical Solver: dof = 32967, time step = 0.25 ms

Prec.	*Newton nit*	*Total nit*	*GMRES it*	*Total it*	*time cpu*	*Tot cpu*
AMG	3	7031	796	6.5 ML	28.42s	15h 47m

Bidomain solver: dof = 9 655490, time step = 0.05 ms

Prec.	κ_2	CG_{it}	$Total_{it}$	$time_{cpu}$	$Total_{cpu}$
MAS(4)	6.18	8	81 178	1.54s	4h 16m

κ_2: average condition number per time step

4.5 Better mechanical solvers: BDDC strong scalability

Land - Niederer et al. active tension model

Fixed global mesh on ellipsoidal domain: $385 \times 385 \times 97$

BDDC primal constraints: VE = Vertex + Edges aver.

VEF = Vertex + Edges aver.+ Faces aver.

Mechanical solver - BDDC preconditioner									
	VE			VEF			boomer		
procs	nit	lit	time	nit	lit	time	nit	lit	time
64	1	58	80.1	1	57	82.9	1	80	30.6
128	1	53	28.9	1	47	29.8	1	80	20.7
256	1	88	11.4	1	75	11.6	1	81	14.6
512	1	87	5.5	1	75	5.7	1	79	15.4
1024	1	59	3.7	1	43	3.7	1	80	28.8

Fermi BG\Q

Mechanical model, BDDC weak scalability

Goktepe et al. active tension model
Fixed local mesh on slab domain: $20 \times 20 \times 20$
Fermi BG\Q, nit almost always 1 (not reported)

Mechanical solver - BDDC preconditioner										
	V		VE		VEF		VEm		VEmF	
procs	lit	time	lit	time	lit	time	lit	time	lit	time
256	94	1.0	42	0.9	38	1.1	32	1.2	26	1.2
512	90	1.1	40	1.1	37	1.3	32	1.5	26	1.5
1024	86	1.4	38	1.6	36	1.9	30	2.1	24	2.2
2048	85	2.2	38	2.9	36	3.5	30	3.9	24	4.1
4096	84	5.2	39	6.6	-	-	-	-	-	-
8192	88	16.7	-	-	-	-	-	-	-	-

V = Vertex, E = Edges averages,
F = Faces averages, m = first order edge moments

Mechanical BDDC scalability and quasi-optimality

slab domain | ellipsoidal domain

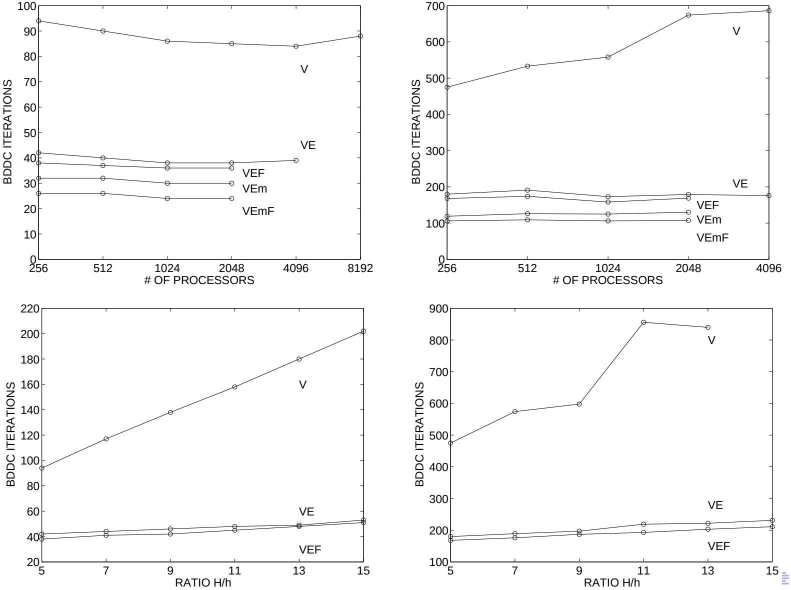

Whole beat: mechanical BDDC with Land-Niederer T_a

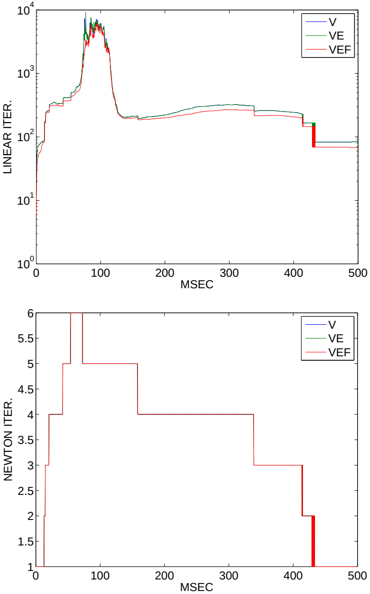

5. Applications: epicardial APD distributions

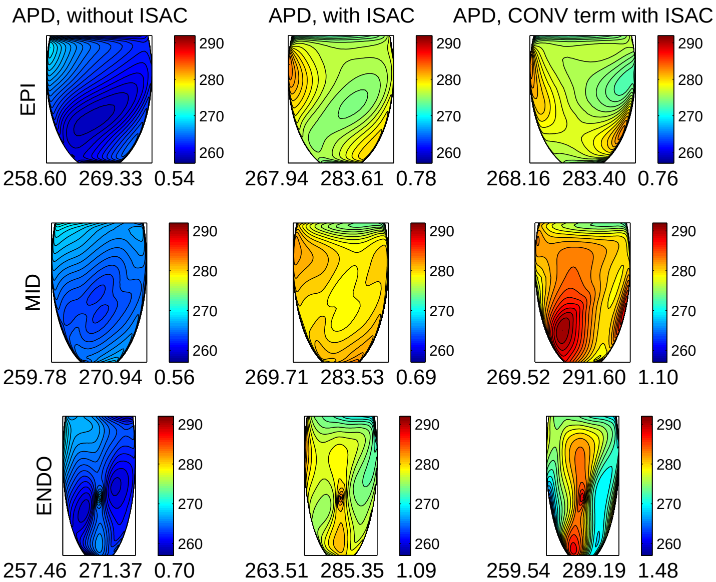

Transmural APD distributions

without ISAC

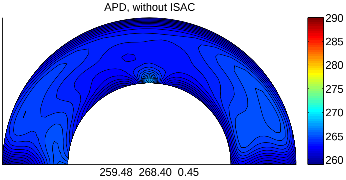

with ISAC

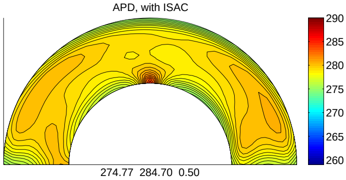

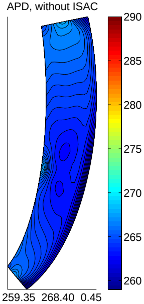

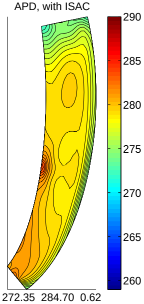

Epicardial waveforms (at apex)

without ISAC (black), with ISAC (red), with CONV + ISAC (blue)

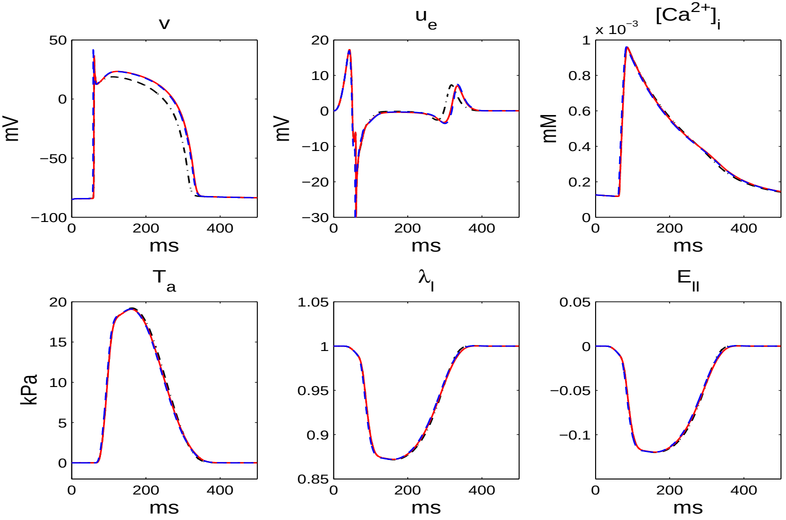

Conclusions

We have developed:

Conclusions

We have developed:

- scalable and efficient Bidomain solvers using domain decomposition preconditioners (multilevel Schwarz). Decoupled NKS and IMEX methods seem more efficient than fully implicit methods.

Conclusions

We have developed:

- scalable and efficient Bidomain solvers using domain decomposition preconditioners (multilevel Schwarz). Decoupled NKS and IMEX methods seem more efficient than fully implicit methods.
- cardiac electromechanical models with transversely isotropic or orthotropic strain energy functions of exponential type; mechanical solvers (Newton-Krylov) using AMG not quite scalable, better performance with DD preconditioners

Conclusions

We have developed:

- scalable and efficient Bidomain solvers using domain decomposition preconditioners (multilevel Schwarz). Decoupled NKS and IMEX methods seem more efficient than fully implicit methods.
- cardiac electromechanical models with transversely isotropic or orthotropic strain energy functions of exponential type; mechanical solvers (Newton-Krylov) using AMG not quite scalable, better performance with DD preconditioners

Complex choice of proper submodel: ionic model, calcium dynamics, Bidomain/Monodomain, active tension, mechanical constitutive law; it depends on competing needs, e.g. biophysical accuracy vs. computational costs

Current/future work

- Study of proper coupling/decoupling strategy of submodels in order to increase numerical stability/efficiency
- effects of electromechanical feedback, stretch-activated channels, convective term on electrical quantities (mostly REPO, APD, T-wave, etc.)
- applications to reentry genesis/termination: shock waveform (mono/biphasic), energy,...
- coupling with haemodynamical models, in collaboration with A. Quarteroni's groups at MOX and EPFL

Current/future work

- Study of proper coupling/decoupling strategy of submodels in order to increase numerical stability/efficiency
- effects of electromechanical feedback, stretch-activated channels, convective term on electrical quantities (mostly REPO, APD, T-wave, etc.)
- applications to reentry genesis/termination: shock waveform (mono/biphasic), energy,...
- coupling with haemodynamical models, in collaboration with A. Quarteroni's groups at MOX and EPFL

THANK YOU

Well-posedness of the Bidomain Model

Difficult degenerate nonlinear parabolic system. For reaction term of FitzHugh-Nagumo (FHN) type:

- rigorous homogenized derivation of the Bidomain model from a periodic assembling of cellular model: Pennacchio, Savaré, Colli Franzone. SIAM J. Math. Anal. 2006.
- ex. & uniq. of Bidomain Pb: Colli Franzone, Savaré: in Evolution equations, Semigroups and Functional Analysis, A. Lorenzi and B. Ruf, (Eds), Birkhauser, 2002 .
- using the parabolic - elliptic Bidomain formulation: Y. Bourgault et al., Nonlin. Anal., 2009
- extension to nonlinear monotone diffusion and time-space dependent reactions of FHN type: M. Bendahmane, K. Karlsen, Netw. Heter. Media, 2006., + Boulakia e al., 2009.

Well-posedness of the Bidomain Model

Difficult degenerate nonlinear parabolic system. For reaction term of FitzHugh-Nagumo (FHN) type:

- rigorous homogenized derivation of the Bidomain model from a periodic assembling of cellular model: Pennacchio, Savaré, Colli Franzone. SIAM J. Math. Anal. 2006.
- ex. & uniq. of Bidomain Pb: Colli Franzone, Savaré: in Evolution equations, Semigroups and Functional Analysis, A. Lorenzi and B. Ruf, (Eds), Birkhauser, 2002 .
- using the parabolic - elliptic Bidomain formulation: Y. Bourgault et al., Nonlin. Anal., 2009
- extension to nonlinear monotone diffusion and time-space dependent reactions of FHN type: M. Bendahmane, K. Karlsen, Netw. Heter. Media, 2006., + Boulakia e al., 2009.

For more general ionic current membrane dynamics, i.e. Hodgkin-Huxley, Luo-Rudy 1 and partially LR2, LRd00 models: M. Veneroni, Nonlin. Anal. 2009.

Well-posedness of the electro-mechanical system

- For a passive, strongly elliptic, store-energy function W^{pas} and for simplest active tensions $T_a = T_a(t, Ca_i)$ (stretch and stretch-rate independent) then the mechanical model is well-posed.
- For general active tension models, the well-posedness of the mechanical model is an open problem,
- The well-posedness of the electro-mechanical coupled model is an open problem.

New book from Springer